Stem Cell Rev and Rep (2018) 14:262–276
DOI 10.1007/s12015-017-9776-7

Evidence of Extracellular Vesicles Biogenesis and Release in Mouse Embryonic Stem Cells

Lilian Cruz[1] · Jenny Andrea Arevalo Romero[1] · Mariana Brandão Prado[1] · Tiago G. Santos[2] · Marilene Hohmuth Lopes[1]

Published online: 14 October 2017

Abstract Extracellular vesicles (EVs) released by mouse embryonic stem cells (mESCs) are considered a source of bioactive molecules that modulate their microenvironment by acting on intercellular communication. Either intracellular endosomal machinery or their derived EVs have been considered a relevant system of signal circuits processing. Herein, we show that these features are found in mESCs. Ultrastructural analysis revealed structures and organelles of the endosomal system such as coated pits and endocytosis-related vesicles, prominent rough endoplasmic reticulum and Golgi apparatus, and multivesicular bodies (MVBs) containing either few or many intraluminal vesicles (ILVs) that could be released as exosomes to extracellular milieu. Besides, budding vesicles shed from the plasma membrane to the extracellular space is suggestive of microvesicle biogenesis in mESCs. mESCs and mouse blastocyst express specific markers of the Endosomal Sorting Complex Required for Transport (ESCRT) system. Ultrastructural analysis and Nanoparticle Tracking Analysis (NTA) of isolated EVs revealed a heterogeneous population of exosomes and microvesicles released by mESCs. These vesicles contain Wnt10b and the Notch ligand Delta-like 4 (DLL4) and also the co-chaperone stress inducible protein 1 (STI1) and its partner Hsp90. Wnt10b and Dll4 colocalize with EVs biogenesis markers in mESCs. Overall, the present study supports the function of the mESCs endocytic network and their EVs as players in stem cell biology.

Keywords Mouse embryonic stem cells · Extracellular vesicles · Vesicles biogenesis · Endosomal trafficking · Transmission electron microscopy

Introduction

Embryonic stem cells (ESCs) are generally derived from the inner cell mass (ICM) of the pre-implantation embryo and are extensively used as a model to study the early mammalian development. ESCs are characterized by three peculiar features: pluripotency, self-renewal and limitless proliferation. The conservation of a pluripotent state is the result of a reciprocal effect between several signaling pathways such as transcriptional regulation circuitry, epigenetic control of gene expression, and singular cell cycle maintenance [1–3].

Within their microenvironment, ESCs are sensitive to multiple signals and play roles that collectively regulate their fate and their function in a spatiotemporal manner. These extrinsic cellular factors include soluble and immobilized factors, extracellular matrix molecules as well as signals presented by neighborhood cells. The adequate presentation of these numerous regulatory signals is necessary for the correct tissue development and homeostasis [4–7]. Thus, the ESCs phenotype is continuously adjusted by the specific conditions of the microenvironment in which they are inserted.

There is growing evidence indicating a role for vesicles released by different cell types to the extracellular environment as carriers of signaling molecules, including proteins, lipids and small RNAs [8–10]. These extracellular vesicles (EVs) are considered novel members of cellular

✉ Marilene Hohmuth Lopes
marilenehl@usp.br

[1] Laboratory of Neurobiology and Stem Cells, Department of Cell and Developmental Biology, Institute of Biomedical Sciences, University of São Paulo, Av. Prof. Lineu Prestes, 1524 - Room 431, 05508-000, Sao Paulo, Brazil

[2] International Research Center, A.C. Camargo Cancer Center, 02056-070 Sao Paulo, Brazil

microenvironment because they can regulate specific intracellular signaling modulating target-cell phenotype, and function. These EVs include the most common defined nomenclatures, exosomes and microvesicles, that differ based on their biogenesis processes and biophysical properties, such as size and content [11].

Exosomes are small homogenous particles sizing between 40 and 100 nm in diameter and are derived from the recycle endocytic pathway. They are intraluminal vesicles (ILVs) found inside of multivesicular bodies (MVBs) that can fuse with the plasma membrane and release their ILVs to the extracellular milieu as exosomes or be directed to degradation through lysosomes. The microvesicles are a more heterogeneous population, sizing 50 to 1000 nm in diameter and are produced through direct budding from the plasma membrane, thus carrying the same components found in the original cell membrane [12–16].

Although many efforts have been made to explain stem cell plasticity based on external signaling molecules, receptors, and target gene activation, some evidence suggest that signal transduction mediated by endosomes-like compartments and/or endosome-associated proteins may play a relevant role in intracellular signal amplification and regulation [17–20]. Hence, investigating the role of EVs from ESCs as microenvironment modulators and how the endocytic machinery works in ESCs may help elucidating the mechanisms required to control stem cell plasticity and reprogramming.

Here, we present ultrastructural and biochemical evidence of vesicles biogenesis machinery in mouse ESCs (mESCs) and blastocysts and highlight the importance of the endocytic processes and the participation of EVs as potential players of stemness and cell fate commitment.

Materials and Methods

Cell Culture

E14.Tg2a mES cell line derived from *Mus Musculus* strain 129/Ola3 (American Type Culture Collection, ATCC; CRL-1821) was cultivated in a feeder cell independent manner. The pluripotency status of this cell line was confirmed by immunofluorescence reaction, qPCR, western blotting, alkaline phosphatase staining and teratoma formation (data not shown). Briefly, cells were maintained on 0.1% gelatin-coated tissue culture dishes in GMEM (Invitrogen) medium supplemented with 2 mM glutamine, 1 mM sodium pyruvate, 1% nonessential amino acids, 15% Fetal Bovine Serum (FBS, Gibco), 50 µM ß-mercaptoethanol, penicillin/streptomycin (1%) and 1000 U/ml Leukemia Inhibitory Factor (ESGRO® LIF; Millipore, Billerica, MA), pH7.4, at 37 °C in a water-saturated atmosphere containing 5% CO_2. For conditioned medium preparation, FBS were ultracentrifuged at 100,000 g for 16 h for extracellular vesicles depletion [21] and used to prepare the medium as described above.

Mouse Embryos Collection

Mice from both C57BL/6 and C57BL/6-Ola background were used for embryos collection. Briefly, 3.5-d.p.c pregnant mice were euthanized and the uterus removed. The uterine horns were flushed with HBSS into a Petri dish. The flushed embryos at late blastocyst stage were collected by using a mouth pipette and transferred to a paraformaldehyde (PFA) 4% solution for fixation. The current study was approved by the Ethical Committee for Animal Research of Institute of Biomedical Sciences, University of Sao Paulo (protocol number 21/2013).

Isolation of EVs from mESCs Medium

Conditioned medium was prepared as previously described [21]. Briefly, E14.Tg2a cells, grown in 100 mm culture dishes, were washed three times with phosphate-buffered saline (PBS) and cultured in 15% exosome-depleted serum containing medium for 48 h. The supernatant was collected on ice and pre-cleared by centrifugation (300 *g* for 10 min, 2,000 *g* for 10 min, and 10,000 *g* for 30 min). Purification of EVs was done by ultracentrifugation at 100,000 *g* for 70 min in an SW40Ti rotor (Beckman-Coulter, Brea, CA, USA). The pellet from ultracentrifugation was resuspended in PFA 4% for electron microscopy processing, in RIPA buffer for immunoblotting analysis.

Immunoblotting Analysis

E14.Tg2a cells lysate were performed using RIPA buffer (50 mM Tris HCl pH7.5; 150 mM NaCl; 2 mM EDTA; 0.5% Triton; 0.5% Sodium Deoxycholate) plus a protease inhibitor cocktail. The same buffer was used to resuspend EVs pellet, but EVs protein extract was not submitted to protein quantification. Cellular protein extract was quantified by the Bradford method with bovine serum albumin as the standard curve. Protein extract (4, 20 and 25 µg) in sample buffer were separated by SDS–PAGE on a 10% polyacrylamide gel at a constant voltage of 120 V and transferred onto a nitrocellulose membrane in a semi-dry system (Trans-Blot Turbo System, Bio-Rad) for 7 min at constant amperage of 1.3 mA. For membrane blocking, 5% non-fat milk and 0.1% Tween 20 in TBS was added for 1 h under agitation at room temperature. The membranes were then incubated with primary antibodies rabbit anti-flotilin (Abcam), mouse anti-HSP90 (Cell Signaling), rabbit anti-Alix, mouse anti-Tsg101 (Sigma), goat anti-Wnt10b (Santa Cruz), rabbit anti-DLL4 (Abcam) or rabbit anti-STI1 [22] overnight at

4 °C. Membranes were then washed and probed with the respective peroxidase-conjugated secondary antibodies (Invitrogen, Life Technologies), for 1 h under agitation at room temperature. Reactions were developed using ECL (GE Life Sciences, Uppsala, Sweden), and membranes were exposed to Hyperfilm (GE).

Immunofluorescence Assay

For immunodetection of pluripotency and endosomal trafficking machinery markers, E14.Tg2a cells were grown in Ibidi-Treat µ-slide (Ibidi, Martinsried, Germany) for 48 h. Cells or embryos were fixed with 4% paraformaldehyde/sucrose in PBS for 15 min, washed three times with PBS and then incubated for 1 h in a blocking solution containing 5% BSA, 0.3% Triton-X 100 diluted in PBS. Samples were incubated overnight at 4 °C with primary antibodies raised against mouse anti-Oct3/4 (Santa Cruz), rabbit anti-Nanog (Cell Signaling), mouse anti-SSEA1 (Cell Signaling), mouse anti-LBPA (Echelon), mouse anti-Alix, rabbit anti-Rab5, rabbit anti-flotilin (Abcam), rabbit anti-VPS36 (Abcam), rabbit anti-Rab27b (Sigma), rabbit anti-VPS4 (Sigma), mouse anti-CD63 (Millipore), goat anti-Wnt10b (Santa Cruz), mouse anti-CD9 (Millipore), rabbit anti-DLL4 (Abcam), mouse anti-Tsg101 (Sigma) or rabbit anti-SHH (Cell Signaling). Samples were washed three times with PBS, followed by 1 h incubation with the respective secondary conjugated with Alexa Fluor-488, -546, -633 or -647 (Thermo Fisher Scientific). Counterstaining of cell nuclei was achieved with 0.1% of 49,6-diamidino-2 phenylindole (DAPI) or TO-PRO-3. After washing with PBS, embryos were kept in PBS and the slides wells were covered with anti-fade solution (glycerol:PBS pH9, 9:1) and examined on an Axio Vert. A1 Carl Zeiss epifluorescence microscope (Zeiss, Aalen, Germany) or on a confocal microscope (Leica TCS SP2 or Zeiss LSM 780-NLO Multiphoton). Images were analysed using LSM software (Zeiss) or ImageJ (NIH).

Transmission Electron Microscopy

E14.Tg2a cells were cultured in ACLAR® Film pre-treated with poli-L-lysine (50 µg/mL) for 48 h. Cells were fixed in a mix of 1:1 medium:2.5% glutaraldehyde in 0.1M cacodylate buffer (pH 7.2) for 15 min at room temperature, and then in 2.5% glutaraldehyde in 0.1M cacodylate buffer (pH 7.2) for 2 h. Briefly, samples were post-fixed in 1% osmium tetroxide in 0.1 M cacodylate buffer (pH 7.2) and dehydrated in a graded series of ethanol at 4 °C. Samples were embedded with ethanol/epon mixtures and polymerized in pure Epon at 60 °C. Ultrathin sections were stained with uranyl acetate and lead citrate. Samples were observed in a Jeol 100 CX II transmission electron microscope from Electron Microscopy Center of Federal University of São Paulo (CEME, UNIFESP) or Department of Cell and Developmental Biology, Institute of Biomedical Sciences of University of São Paulo (ICB-USP) or Department of Biomaterials and Oral Biology, School of Dentistry (USP).

EVs obtained from ultracentrifugation were deposited onto Formvar-carbon-coated electron microscopy grids, fixed with a mixture of 2% paraformaldehyde and 0.125% of glutaraldehyde. Samples were contrasted and embedded in a mixture of methylcellulose and uranyl acetate, and observed under a Jeol 100 CX II transmission electron microscope from CEME.

EVs Size and Quantification

Cells were cultured for 48 h with EVs-depleted medium and conditioned media were centrifuged as previously mentioned before analysis. The particle number and size of EVs was counted by a Nanoparticle Tracking Analysis (NTA) device (Nanosight LM20, coupled to a CCD camera and a laser emitting a 60-mW beam at 405- nm wavelength).

RNA Detection and Quality

RNA from mESCs and EVs was isolated using Trizol (Invitrogen, Paisley, UK) according to the manufacturer's protocol. Detection, quality, and size of RNA were performed using capillary electrophoresis (Agilent RNA 6000 Nano Kit for mESCs RNA and EVs RNA and Agilent Small RNA Analysis Kit for EVs RNA) according to the manufacturer's protocol (Agilent 2100 Bioanalyzer®, Agilent Technologies, Foster City, CA, USA).

Results

Ultrastructural Analysis of ESCs Morphology

Since little is known about the ultrastructure of mESCs, we first evaluated their main structural features in detail using transmission electron microscopy (TEM). Consistent to that observed by light microscopy during the routinely maintenance of mESCs (Fig. 1a), these cells grow in an adherent monolayer way forming isolated colonies (Fig. 1b, c). This morphology was preserved due to the use of a specific membrane (ACLAR Film) for mESCs plating to EM processing. Different stages of cell cycles were observed in a single colony. For instance, we observed some nuclei with highly condensed chromatin and other nuclei with evident euchromatin, heterochromatin and nucleolus (Fig. 1b, c, d).

The mESCs present a large nucleus that occupies most part of the intracellular space with a scarce cytoplasm (Fig. 1d). We also observed numerous mitochondria distributed across the cytoplasm (Fig. 1b) and a well-preserved

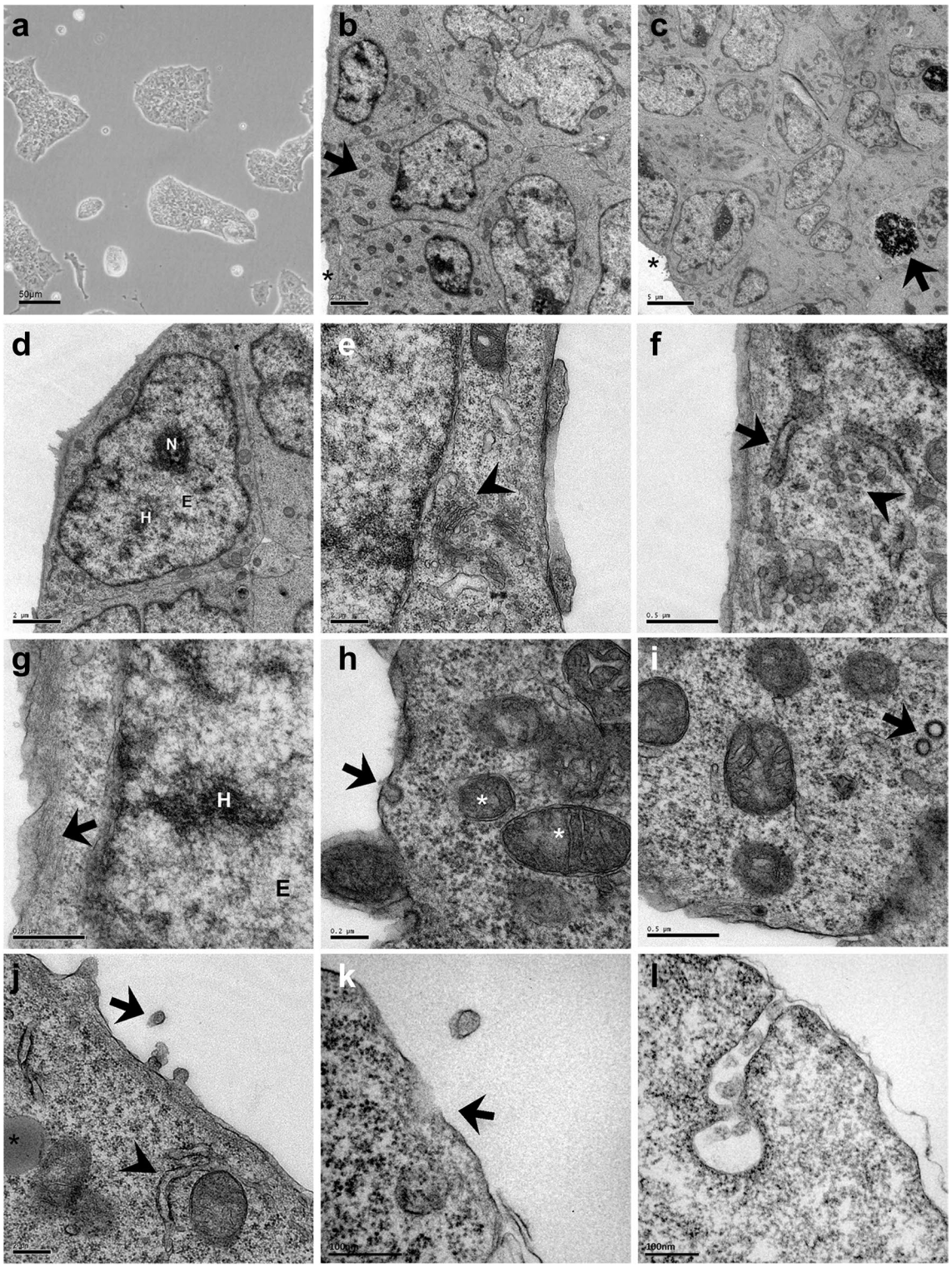

peripheral cytoskeleton architecture represented by an actin-rich layer in cell cortex (Fig. 1g).

Ultrastructural Analysis of Endocytic Events in ESCs

We next focused on describing the ultrastructure of endocytic pathways and intracellular vesicle trafficking. The Golgi apparatus was clearly visible with its cisternae and

◂**Fig. 1** Ultrastructural analysis of mouse embryonic stem cells (mESCs). **a**-**d**: Overview of mESCs characteristics. **a** Light microscopy image from a routinely mESCs culture showing the isolated colonies formed after 48 h. **b** and **c** Overview of a mESCs group near the colony border (asterisc). Note mitochondria (*arrow* in **b**) and mitotic events in some cells (*arrow* in **c**). **d** Zoom in on an ESC colony. Note the high nucleus:cytoplasm ratio (N = nucleolus, H = heterochromatin, E = euchromatin). **e** Golgi apparatus with organized cisternae and transport vesicles (*arrow* head). **f** Vesicles (*arrow* head) near rough endoplasmic reticulum (RER) (*arrow*). **g** Preserved cytoskeleton architecture in membrane vicinity (*arrow* indicates actin-rich layer). **h-l** Endocytosis and/or exocytosis events. **h** Coated pits indicating clathrin-mediated endocytosis (*arrow*). Note mitochondria with round and oval shape (asterisc). **i** Coated vesicles in the cytoplasm (*arrow*). **j** and **k** Shedding vesicles from the plasma membrane. **j** Budding of vesicles (*arrow*). Note the RER (*arrow* head) and a lipid droplet (asterisc). **k** Moment of vesicle release. Note the membrane integrity deformation (*arrow*), possibly due to microvesicle budding. **l** Uptake or release of vesicles. Scale bars: **a**: 50 μm; **b**, **d**, **e**, **j**: 2 μm; **c**: 5 μm; **f**, **g**, **i**: 0.5 μm; **h**: 0.2 μm; **k**, **l**: 100 nm

vesicles distributed in its vicinity (Fig. 1e) and near to the nucleus and to the rough endoplasmic reticulum (RER) (Fig. 1f).

Clathrin-mediated endocytosis was often seen in the plasma membrane and clathrin-coated endocytic vesicles were seen in the cytoplasm (Fig. 1h, i). In some cells, but not all, we noted events related to the release of vesicles from the plasma membrane (Fig. 1j, k), which could be referred to as microvesicles. In some cases, we noticed a small region showing disruption of the cell membrane near the EV, suggesting that it has just been budded from the membrane (Fig. 1k). This phenomenon suggests a mechanism of microvesicles formation. Events that resemble vesicles uptake were also observed in these cells (Fig. 1l) indicating that mESCs may use EVs as intercellular communication and as a way to sense their microenvironment.

Since the endosomal network is evident and active in these cells, we looked for MVBs, which are structures related to exosomes biogenesis. As shown in the panels of the Fig. 2 (a-i), strong evidence of the presence of MVBs in mESCs were found. MVBs are spherical and limited by a double membrane and contain ILVs generated by invagination and scission from the limiting membrane of the endosome. MVBs may either fuse with lysosome to be degraded or may fuse with the plasma membrane in which case they release ILVs to the extracellular environment and become exosomes. MVBs contain a variable number of ILVs and are surrounded by and connected with tubular compartments (Fig. 2c, d, h). The tubular extension connects the MVBs to endosomal protein sorting compartments, as evidenced by the proximity to RER and polyribosomes (Fig. 2b, d, h). We also noted the presence of vesicles in their vicinity (Fig. 2c, d, e, h). In some cases, we observed endosomal structures with heterogeneous content consisting of many ILVs together with other lamellar and electron dense structures (Fig. 2j, k, l). Indeed, during the early steps of the endocytic pathway, ILVs are small and homogeneous in size, but intraluminal membranes become pleiomorphic in late endosomes. Inside them, ILVs can combine with onion-like lamellae in merged multivesicular-multilamellar regions or domains [23, 24]. These events explain the presence of some MVBs carrying heterogeneous content, which actually illustrate the pleiomorphic nature of late endosomes.

Altogether, this detailed ultrastructural analysis of mESCs confirms the presence of both exosomes and microvesicles biogenesis, supporting a role for these EVs in ESCs biology.

EVs Biogenesis Machinery in mESC and Mouse Blastocyst

The specific expression of classical transcription factors confirmed the pluripotency status of mESCs cell line used in this study (Fig. 3a, b). mESCs express Oct4, Sox2 and Nanog in the nucleus and SSEA1 on their surface (Fig. 3a). We next evaluated specific molecular markers for the biogenesis machinery in mESCs and mouse embryos through immunofluorescence. The generation of ILVs inside MVBs involves the action of components of the *Endosomal Sorting Complex Required for Transport* (ESCRT) [25–27]. Vacuolar protein sorting 36 (VPS36), a member of ESCRT-II complex, and Rab27b, a small GTPase that acts in the vesicle transport to the membrane [28, 29], presented a punctate distribution throughout the mESCs cytoplasm (Fig. 3c). Vacuolar protein sorting 4 (VPS4), which is an accessory protein of ESCRT machinery, was found diffused in the cytoplasm when we expected to find it in a punctate form (Fig. 3c).

The unconventional lipid lysobisphosphatidic acid (LBPA), abundant in ILVs of late endosomes but not found in early endosomes [30, 31], was observed in the perinuclear region of mESCs, having either positive or negative cells in the same colony (Fig. 3c).

In order to confirm the pattern of distribution of endocytic markers presented in mESCs we used freshly collected mouse embryos at early developmental stage (E3.5). This stage corresponds to the late blastocyst which contains the trophectoderm and the ICM from where ESCs can be derived. VPS4 and Rab27b presented same pattern as seen in mESCs (Fig. 4). In addition, Alix, an ESCRT acessory protein, flotilin, a protein involved in endosomal trafficking events, and Rab5, a Rab GTPase associated with the sorting endosome and with endosomal fusion events, were also visualized in the embryos, not only in ICM but also in trophectoderm (Fig. 4).

The expression of these components, which associate to vesicle biogenesis and trafficking, strengthen the need to consider the dynamic of endosomal compartmentalization for ESCs function and for early developmental events.

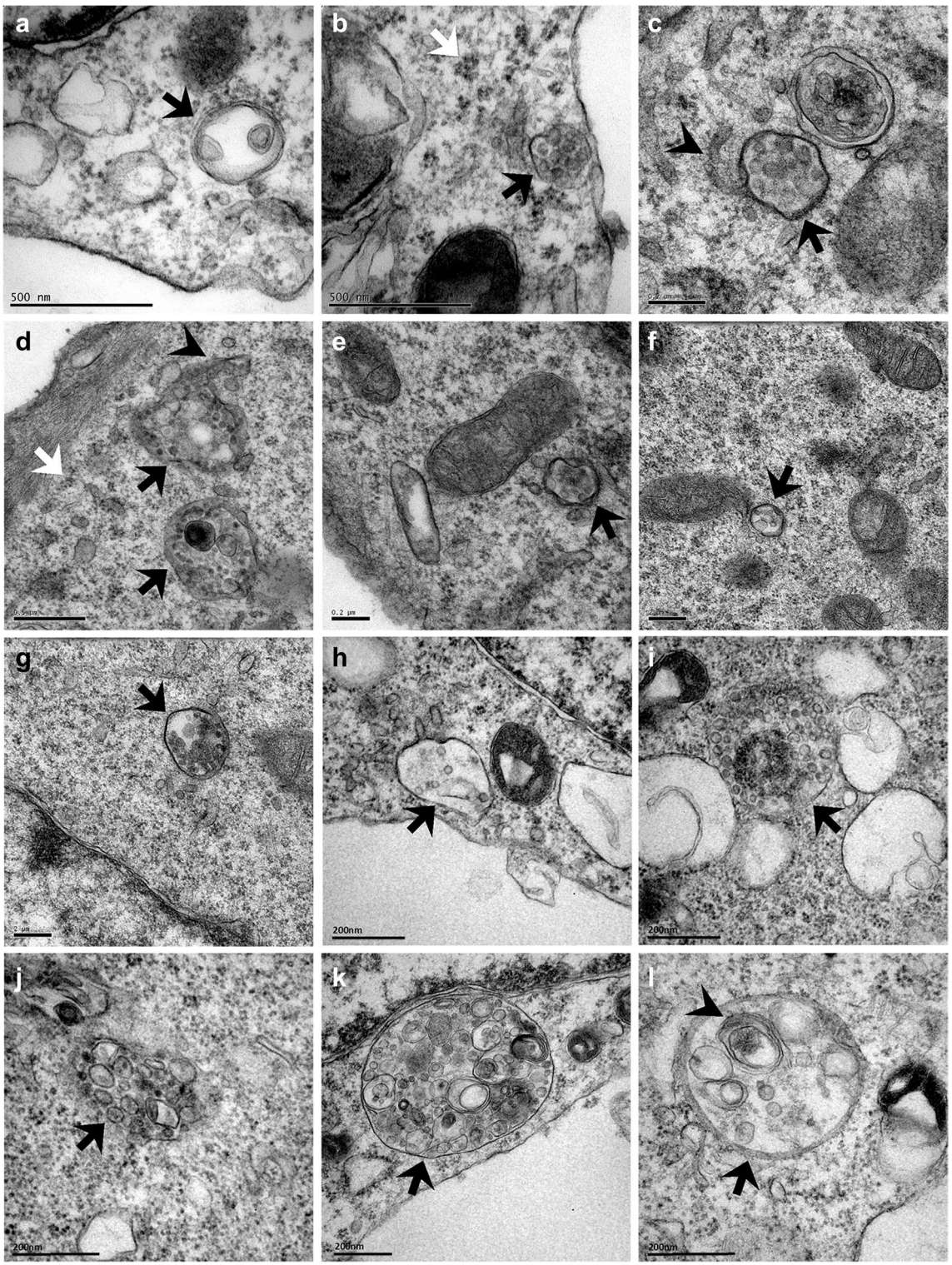

Fig. 2 Ultrastructural evidence of multivesicular bodies (MVBs) and late endosomes. **a** Double membrane MVB (*arrow*) with two cup-shaped double membrane intraluminal vesicles (ILVs). **b** MVB near the plasma membrane (*black arrow*). Polyribosomes indicated by white arrow. **c** MVB (*arrow*) with tubular extension (*arrow* head). **d** Two MBVs (*arrows*) with high amount of ILVs. Note the tubular extension of the MVB on the top (*arrow* head). White arrow: Polyribosomes. **e, g** and **h** MVB (*black arrow*) with surrounding vesicles. **f** MVB (*arrow*) with few ILVs. **i-l**: MVB (*arrow*) with high quantity of ILVs and more pleiomorphic shape. **k-l**: Lamellar structures (*arrow* head in **l**) and heterogeneous content in MVBs characterize late endosomes. Scale bars: **a**, **b**, **d**: 500 nm; **c**, **e**, **h**–**l**: 200 nm; **f**, **g**: 2 µm

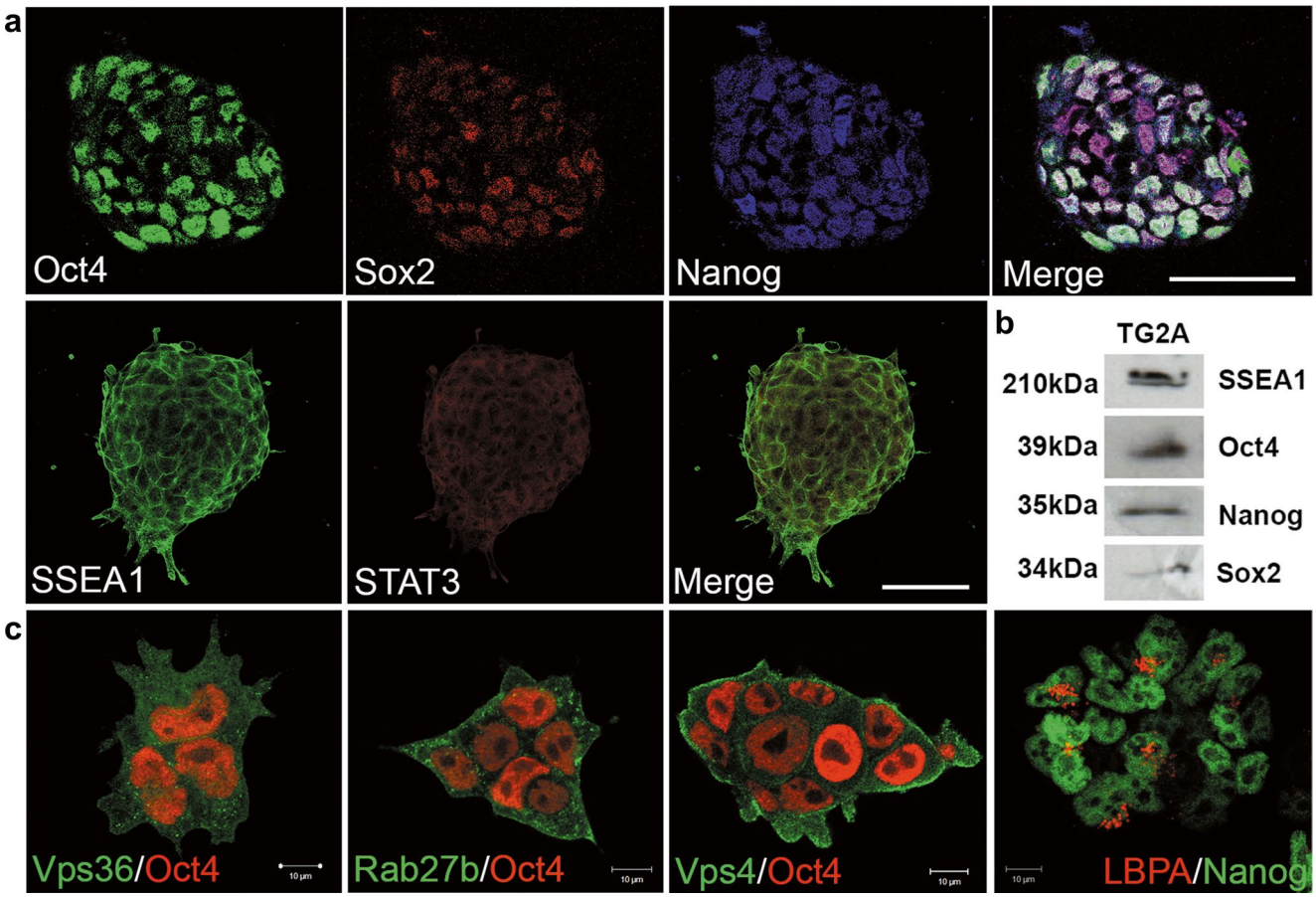

Fig. 3 Machinery of extracellular vesicles (EVs) biogenesis of pluripotent mouse embryonic stem cells (mESCs). **a** mESCs line immunostained with pluripotency related markers, Oct4, Sox2, Nanog, Stat3 and SSEA1. Nuclei were stained with TO-PRO-3. Bars: 50 µm. **b** Immunoblotting detection of pluripotency factors in mESCs line cell extract (10 µg). **c** mESCs were immunostained with anti-vacuolar protein sorting 36 (VPS36), member of ESCRT-II; **b** anti-Rab27b, a Rab GTPase that regulates vesicles exocytosis; **c** anti-vacuolar protein sorting 4 (VPS4), an AAA ATPase that participates of the ESCRT machinery and **d** anti-lysobisphosphatidic acid (LBPA), considered a marker of intraluminal vesicles. Nanog and Oct4 were used as marker of pluripotent state of mESCs. Bars: 10 µm

EVs Profile Released by mESCs

In order to characterize the EVs secreted by mESCs, we used the mESCs medium to isolate EVs through ultracentrifugation protocol according to Théry et al., 2006 [21]. TEM used to verify the ultrastructure of EVs indicated spherical, membrane-surrounded vesicles and revealed a cup-shaped morphology as commonly described for exosomes (Fig. 5a, b). To determine vesicle size variation, we used NTA (Nanosight). This analysis showed that most EVs detected sizes between 50 and 150 nm in diameter (Fig. 5c), indicating vesicles ranging in size for exosomes. Through immunoblotting analysis we confirmed the presence of protein generally found in EVs such as Alix, heat shock protein 90 (HSP90), flotilin and Tsg101 (Fig. 5d). We also confirmed that mESCs EVs carry the co-chaperone stress inducible protein 1 (STI1) (Fig. 5d), as do other EVs from distinct cell types [32]. Ponceau staining revealed differential protein content in nitrocellulose membrane-bound EVs protein extracts compared to mESCs extracts (Fig. 5d). Moreover, mESCs EVs carry the membrane-associated proteins Wnt10b and Notch ligand Delta-like 4 (DLL4), members of the developmental signals WNT and Notch (Fig. 5e). Besides detection of proteins and specific markers, small RNAs were also detected (Fig. 5f). The RNA profile analysis revealed that total RNA from EVs does not contain ribosomal RNA (rRNA) as noted by the absence of the apparent peaks 18S and 28S rRNAs, clearly seen in mESCs total RNA. This assay showed that the majority of total EVs-derived RNA is below 1 kb, revealing that small RNAs are abundant in mESCs derived EVs (Fig. 5f).

Since Wnt10b and DLL4 were present in mESCs EVs, their intracellular distribution and potential association with vesicles biogenesis markers were addressed in mESCs by immunofluorescence. Wnt10b and DLL4 partially colocalized with CD9, CD63, Tsg101 or Vps36 (Fig. 6) suggesting

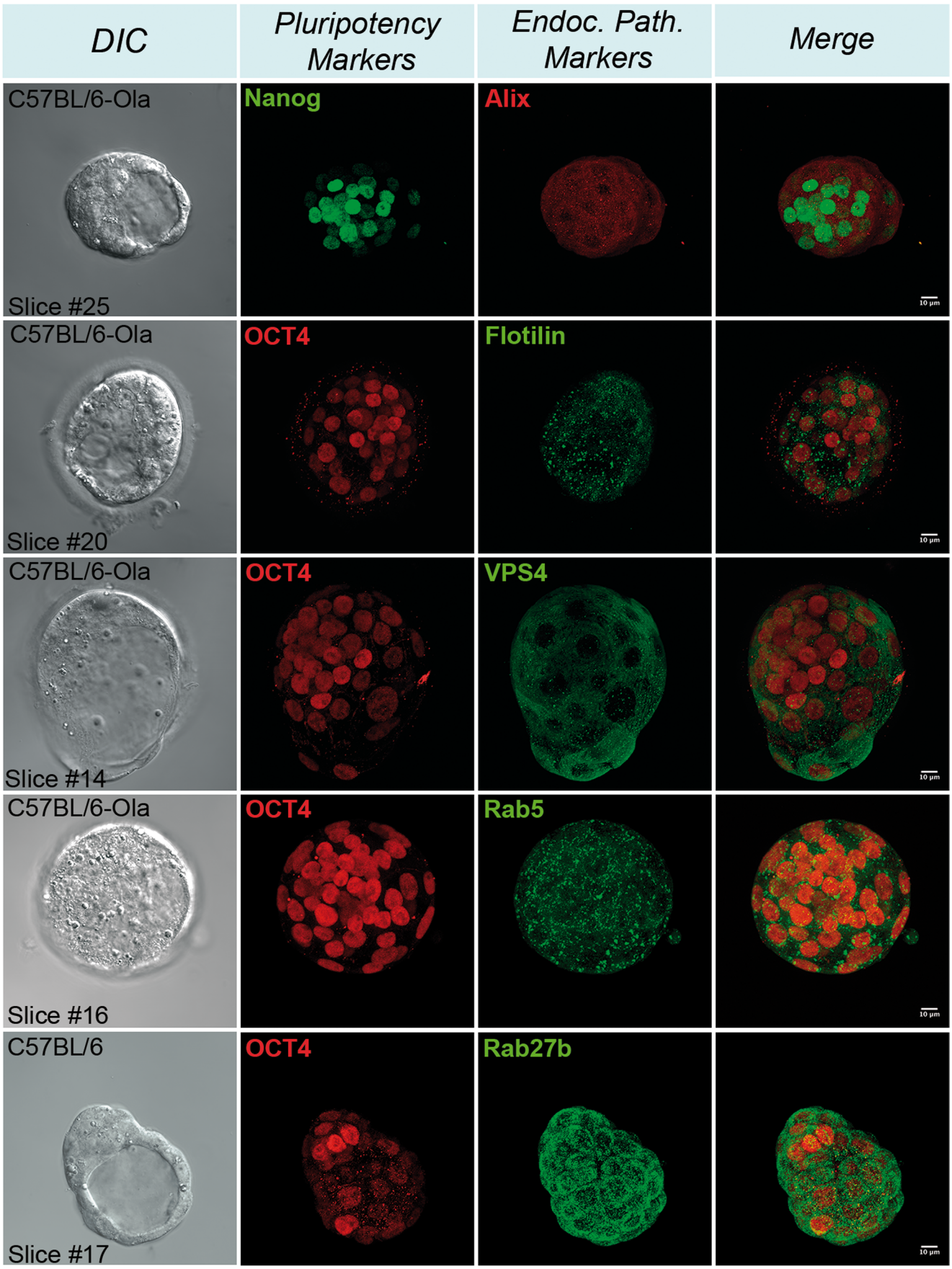
DIC
Pluripotency Markers
Endoc. Path. Markers
Merge
C57BL/6-Ola
Slice #25
Nanog
Alix
10 µm
C57BL/6-Ola
Slice #20
OCT4
Flotilin
10 µm
C57BL/6-Ola
Slice #14
OCT4
VPS4
10 µm
C57BL/6-Ola
Slice #16
OCT4
Rab5
10 µm
C57BL/6
Slice #17
OCT4
Rab27b
10 µm

◂**Fig. 4** Extracellular vesicles (EVs) biogenesis markers in mouse embryos. Embryos in blastocyst stage from both C57BL/6 or C57BL/6-Ola background were immunostained with anti-Alix, an ESCRT acessory protein; anti-flotilin, protein involved in endosomal trafficking events; anti-vacuolar protein sorting 4 (VPS4), an AAA ATPase that participates of the ESCRT machinery; anti-Rab5, a Rab GTPase associated with the sorting endosome and endosomal fusion events; anti-Rab27b, a Rab GTPase that regulates vesicles exocytosis. Nanog and Oct4 were used as marker of pluripotent state. Bars: 10 μm

an alternative route of release besides their canonical secretory pathway.

Discussion

Embryonic stem cells have been extensively applied in developmental model studies due to their particular features of pluripotency, self-renewal and unlimited proliferation, which characterize them as highly plastic cells. Many efforts have been made to reveal the molecular mechanism of the pluripotency state of ESCs and cell fate commitment. How these cells sense and process the information from their microenvironment, how they communicate with neighborhood cells and the biological consequences of that and, in which moment and why they choose to commit to a specific phenotype are still unanswered questions that are under intense debate [33–37].

EVs have emerged as important players, transferring information between cells due to their capacity of transporting specific molecules from their origin cell in the autocrine and/or paracrine ways. These molecules involve big molecules such as proteins and bioactive lipids to small RNAs like microRNA that upon target cell uptake may play a role in intracellular signaling such as mRNA silencing or signal networks (in) activation. As for stem cells (embryonic or adult) plasticity, EVs may support a mechanism to regulate target cell phenotype, which in turn leads to cell fate choice and cell fate switching [38–41].

Although additional studies are needed to define molecular mechanisms of EVs biogenesis and their biological significance in mESCs, our study reveals enhanced ultrastructural details of EVs biogenesis and their release by mESCs *in vitro*. Our initial ultrastructural analysis of mESCs showed that these cells presented a high nuclei:cytoplasm ratio, with the nuclei with abundant euchromatin and a sparse heterochromatic region. The colony of mESCs formed *in vitro* displayed some cells in mitosis showing the mESCs proliferative feature. Lipid droplets were rarely seen in the cytosol. The cytoplasm was characterized by many mitochondria, varying from small rounded with few transverse cristae to more egg shaped and pleiomorphic ones. The cells showed prominent RER with polyribosomes in the cytoplasm, as well as smooth endoplasmic reticulum and Golgi complexes with secretory vesicles (Fig. 1). These characteristics strongly support the high capacity of protein synthesis and secretion and metabolic activity of mESCs. Furthermore, other components of the endosomal trafficking system were revealed by the presence of coated pits and vesicles, indicating occurrence of clathrin-mediated endocytosis; MVBs with low or high quantities of ILVs resembling early, transient or late endosomes; MVBs with multilamellar and multivesicular content resembling late endosomes; and MVBs with tubular extensions that connect them to endosomal protein sorting compartments (Figs. 1 and 2) [42, 43]. In fact, the MVBs are also considered a source of ILVs that are released as exosomes upon fusion of MVBs with the plasma membrane. Therefore, both the presence of MVBs, and the apparent budding vesicles that shed from the plasma membrane into the extracellular milieu, and the EM of isolated EVs strongly support the feature of ESCs as a potential source of exosomes and microvesicles, which in turn can play a role on intercellular communication during early development.

Besides their direct involvement with EVs biogenesis, components of the endosomal transport machinery have been involved to promote spatial and temporal control over specific stem cell signaling networks. For instance, the JAK/STAT pathway activation, among other signaling pathways, that has been implicated in maintenance of the pluripotent status of ESCs does require STAT3 translocation to the nucleus [44–47]. Interestingly, a protein of the endocytic system, Asrij, has been shown to interact with STAT3 [49]. Asrij colocalizes with STAT3 in endosomes and aids STAT3 activation, by which it exerts an essential role on stemness maintenance in mESCs [48]. Another example is Wnt signaling. The canonical Wnt pathway requires inhibition of GSK3 activity, and this inhibition contributes to maintain a pluripotent state of ESCs [49, 50]. Indeed, Taelman et al. [51] showed that Wnt signaling leads to the sequestration of GSK3 from the cytosol into MVBs, which then separates the enzyme and its cytosolic substrates [51].

The cellular distribution of conventional exosome biogenesis pathway was assessed either in the mESCs or in the blastocysts. We observed that VPS36 and Rab27b were apparent throughout the cytoplasm and had a punctate form. VPS4 was diffuse and LBPA was highly expressed and aggregated in the perinuclear region in some cells and in others appeared smaller and spread in the cytoplasm (Figs. 3 and 4). The expression of these molecules supports the presence of the machinery involved in the exosome biogenesis, or at least in the endosomal transport system. Some of these molecules are members of the ESCRT system. ESCRT complexes are composed of four members (ESCRT-0, -I, -II and –III), and other accessory proteins (VPS4, VTA1, ALIX). Briefly, ESCRT-0 acts in the clustering ubiquitinylated cargo

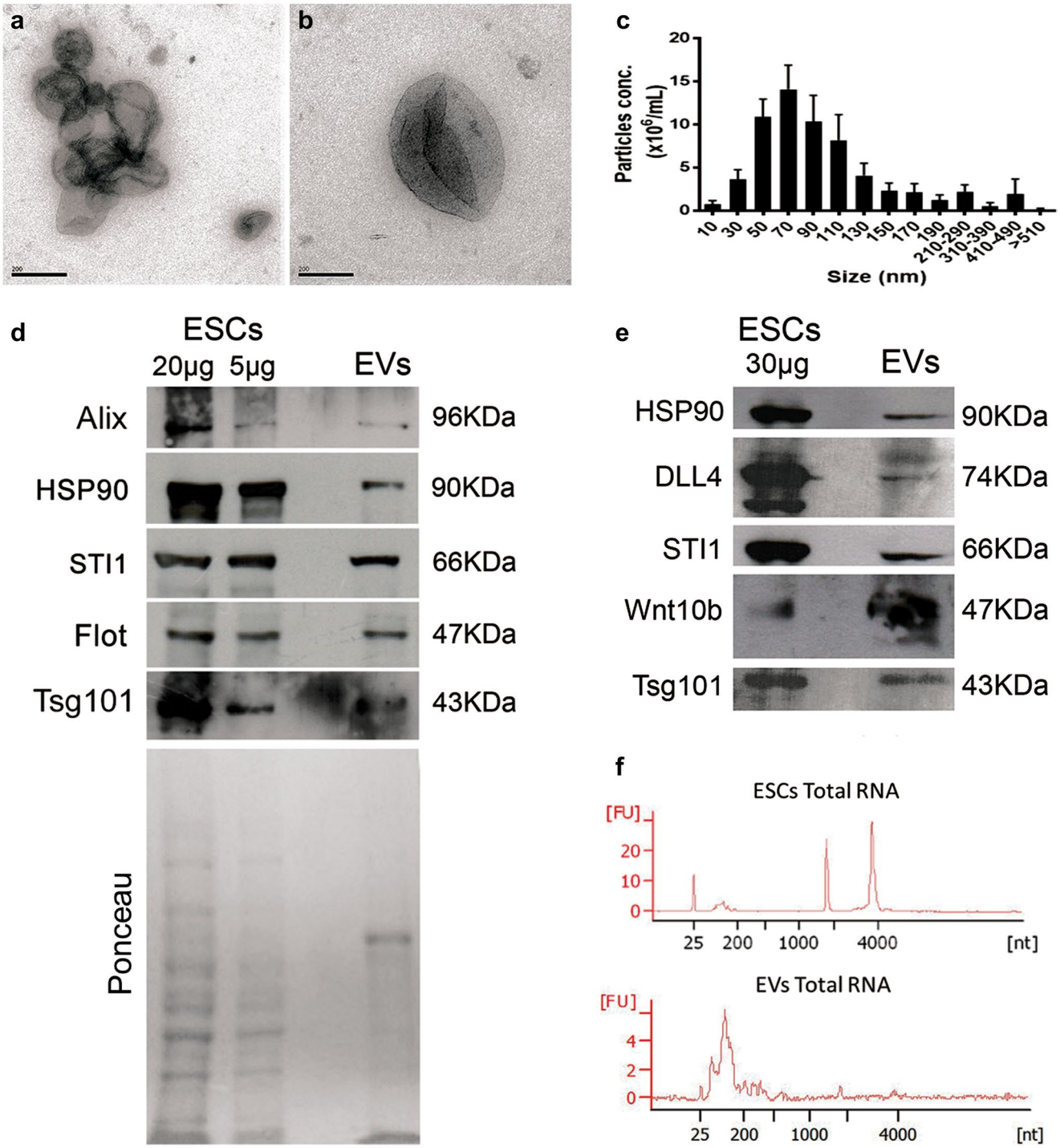

Fig. 5 Characterization of mESCs-derived extracellular vesicles isolated by ultracentrifugation. **a-b**: Ultrastructural morphology showing round double-membrane cup-shaped vesicles. **c** Size and quantification of EVs by NTA technique showing high amount of EVs with diameter ranging from 50 to 150 nm. Bars indicate mean ± SEM for two independent experiments. **d** Immunoblotting detection of Alix, heat shock protein 90 (HSP90), stress-inducible protein 1 (STI1), flotilin and Tsg101 in both cell extract (mESCs) and EVs extract (EVs). Profile of the total protein extracts of mESCs and EVs visualized by the Ponceau staining of the membrane. **e** Immunoblotting for HSP90, DLL4, STI1, Wnt10b and Tsg101 in both cell extract (ESCs) and EVs extract (EVs). **f** Bioanalyzer data of total RNA isolated from mESCs and EVs showing the size distribution of RNA. The two main peaks in mESCs RNA correspond to 18S (1900nt) and 28S (4700nt) ribosomal RNA, respectively. EVs-derived RNA is more enriched in small RNA (peak from 30 to 250nt) and peaks of rRNA are not evident in EVs total RNA. FU: fluorescence units. nt: nucleotides

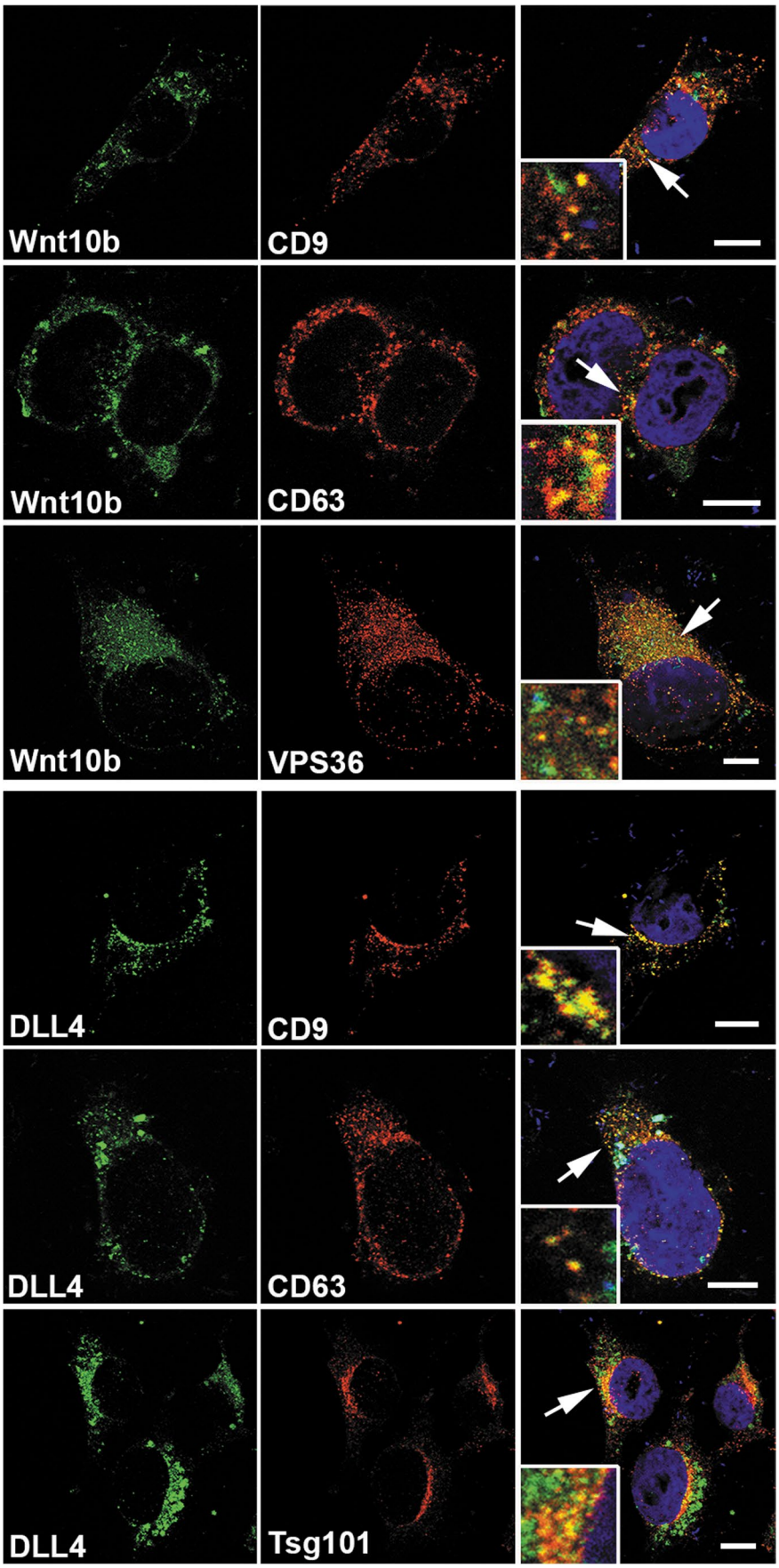

Fig. 6 Exosomes and EVs biogenesis markers co-localize with morphogens in mESCs. mESCs were immunostained with Wnt10b and tetraspanins used as exosome markers (CD9 and CD63) and also anti-vacuolar protein sorting 36 (VPS36), member of ESCRT-II. mESCs were immunostained with DLL4 and CD9, CD63 or VPS36. Nuclei were stained with TO-PRO-3 (in *blue*). Inset shows higher magnification of colocalization area depicted by arrows. Bars: 10 µm

in the endosomal membrane. ESCRT-I (Tsg101, Vps28, Vps37, MVB12, and UBAP1) and ESCRT–II (VPS36, VPS22, VPS25) are responsible for membrane budding whereas ESCRT-III (CHMP 1–7, IST1) cleaves the budded membrane by fission [25–27, 52, 53]. LBPA is an unconventional phospholipid recently found to interact specifically with ALIX and thereby may play a direct role in the ESCRT-dependent ILVs formation within late endosomes [31, 54, 55]. Although it has been described only in ILVs of late endosomes destined to lysosomes [56], one study has shown that LBPA can be present in exosomes as ALIX does [57]. Nevertheless, we cannot state which destination the LBPA-positive ILVs of mESCs may take.

After confirming the existence of EVs machinery in mESCs, the structural analysis of EVs, purified by ultracentrifugation, showed the presence of double-membrane round-shaped vesicles. NTA technology showed that most EVs isolated by the ultracentrifugation protocol used in this study range from 50 to 150 nm. Based on the size, these data suggest that the EVs are mostly exosomes, albeit microvesicles were also detected, which indicates that the isolated EVs correspond to an exosome-enriched heterogeneous population of mESCs EVs.

Furthermore, we showed that mESCs-derived EVs are enriched with small sized RNAs fraction, as observed by a unique peak at Bioanalyzer RNA size profiling (Fig. 5), which could include regulatory non-coding RNAs like miRNAs, piRNAs, snoRNAs, tsRNAs, among others. Additionally, EVs of mESCs expressed documented markers such as flotilin, HSP90, Alix and Tsg101 as expected. STI1 was also present, corroborating previous works that found this co-chaperone in EVs from other cell types such as astrocytes [32]. As a co-chaperone, STI1 regulates HSP90 and HSP70 activity, by binding to both molecules forming a complex responsible for the correct folding of target proteins [58–60]. Likewise STI1, HSP70 and HSP90 are also found in EVs, but it is still unknow if they are complexed inside the EVs. Alternativley, it is possible that STI1 acts as a co-chaperone when released through EVs [61, 62]. Furthermore, STI1 is related to ESCs pluripotency maintenance since it modulates different processes like nuclear translocation of the transcriptional factor STAT3 as well as regulation of embryoid bodies formation from ESCs [63–65]. Thereby, the confirmation of secreted STI1 by mESCs-derived EVs supports the role of this protein in modulating processes related to embryonic development. Altogether, the ultrastructural evidence of isolated EVs and the detection of proteins and the small RNAs enrichment strongly suggest that mESCs-derived EVs underlie or synergize developmental events by acting as carriers of regulatory molecules.

Indeed, some studies have demonstrated the capacity of ESCs-derived EVs to induce epigenetic reprogramming of target differentiated cells, such as adult hematopoietic stem/progenitor cells, murine embryonic fibroblasts, retinal progenitor Muller cells through proteins, mRNA and miRNA delivery [38, 66, 67]. These studies have shown that the horizontal transfer of protein/RNA-based information induces morphological and transcriptional changes towards a more de-differentiated and stemness phenotype. Several evidence pointed out that EVs from different cell sources also carry morphogens and other bioactive molecules important for embryonic development like Wnt, Hedgehog and the Notch-ligand Delta, which were also found in MVBs, therefore supporting a key role for EVs in cell-to-cell communication during embryogenesis [39, 68–71]. These molecules can regulate processes including body axis patterning, proliferation, polarity and migration, stem cell renewal, cell fate specification, among others, during development [72–75]. Supporting the new release mechanism for morphogens, our data confirmed for the first time that mESCs release the specific Wnt and Notch signaling components, Wnt10b and DLL4, respectively, via EVs. Western blot indicates that Wnt10b and DLL4 are expressed in both cell lysates and EVs of mESCs (Fig. 5e). Consistently with the presence in EVs, the intracellular distribution of Wnt10b and DLL4 in mESCs by immunofluorescence revealed their colocalization to some EVs biogenesis markers such as CD9, CD63 and Tsg101 or Vps36 (Fig. 6). DLL4 containing EVs were described to be involved in activation or inhibition of Notch signaling in the recipient cells [76, 77]. DLL4 released by EVs can play a role in cell phenotype switch of endothelial cells by modulating Notch receptor expression [76] and in angiogenic sprouting suppression by inducing the Notch signaling [77]. Wnt signaling members are found in the surface of EVs and are able to activate Wnt signaling in target cells [78]. So far, Wnt10b-containing EVs has only been described in stromal fibroblasts, exerting a paracrine effect in breast cancer cells [79]. More recently, the only work that describes in detail the role of EVs secreted by mESCs at the earliest embryo stage, reveals that mESCs EVs are able to transfer their contents to trophoblasts, to promote trophoblasts migration and to increase the efficiency of the embryos implantation [74].

In summary, we have characterized elements that support the presence of vesicle biogenesis machinery in mESCs. Our data reveal the presence of vesicles biogenesis structures and their molecular markers, and we also showed the nature of isolated EVs. A schematic overview of ESCs-derived EVs as components of ESC microenvironment and their possible target cell effects is illustrated in Fig. 7. Hence, ours findings provide basis for further studies to examine the biological influence of EVs secreted by mESCs during early embryonic development and to unveil the relevance of a highly active endosomal trafficking for stemness signaling circuits in mESCs.

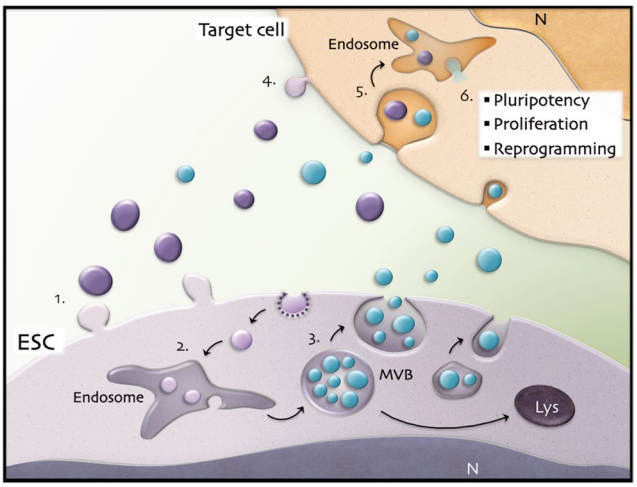

Fig. 7 Extracellular vesicles (EVs) as potential modulators of stem cell niche. EVs include microvesicles (in *purple*) shed from the cell membrane (1), as well as exosomes (in *blue*) found inside multivesicular bodies (MVBs) formed through endocytic pathway (2). MVBs fuse with membrane and release the exosomes (3) or can be directed to degradation through lysosomes. In the microenvironment, EVs can achieve a target cell and deliver their content through plasma membrane fusion (4) or be internalized and fuse with the delimiting membrane of an endocytic compartment (5). The release of their content inside the recipient cell may modulate effects upon stemness status (6). N: nucleus, Lys: lysosome

Acknowledgements We are very grateful to Dr. Vilma R. Martins, Research Superintendent of International Research Center at A. C. Camargo Cancer Center and her group, specially, Marcos Vinicios Salles Dias and Fernanda Giudice for technical support in NanoSight equipment. We also are thankful to Camila Lopes Ramos from Sirio-Libanes Hospital Teaching and Research Institute for technical support in RNA assays. We also thank Mario Costa Cruz (CEFAP-USP, Confocal Microscopy technician); Gaspar Ferreira de Lima, Edson Rocha de Oliveira, Victor E. Arana-Chavez, Márcia Tanakai, André Aguillera and Rita S. (CEME) for technical assistance in electron microscopy.

Compliance with Ethical Standards

Conflict of interest The authors declare that they have no conflicts of interest.

Financial Support This study was supported by Fundação de Amparo a Pesquisa do Estado de São Paulo (FAPESP, Processes numbers: 2011/13906-2, 2013/22078-1 and 2014/17385-5).

References

1. Nichols, J., & Smith, A. (2011). The origin and identity of embryonic stem cells. *Development (Cambridge, England), 138*(1), 3–8.
2. Nichols, J., & Smith, A. (2012). Pluripotency in the embryo and in culture. *Cold Spring Harbor Perspectives in Biology, 4*(8), a008128.
3. Li, M., & Belmonte, J. C. I. (2017). Ground rules of the pluripotency gene regulatory network. *Nature Reviews Genetics*. https://doi.org/10.1038/nrg.2016.156.
4. Quesenberry, P. J., & Aliotta, J. M. (2008). The paradoxical dynamism of marrow stem cells: Considerations of stem cells, niches, and microvesicles. *Stem Cell Reviews, 4*(3), 137–147.
5. Keung, A. J., Kumar, S., & Schaffer, D. V. (2010). Presentation counts: microenvironmental regulation of stem cells by biophysical and material cues. *Annual Review of Cell and Developmental Biology, 26*, 533–556.
6. Camussi, G., Deregibus, M. C., & Cantaluppi, V. (2013). Role of stem-cell-derived microvesicles in the paracrine action of stem cells. *Biochemical Society Transactions, 41*(1), 283–287.
7. Sthanam, L. K., et al. (2017). Biophysical regulation of mouse embryonic stem cell fate and genomic integrity by feeder derived matrices. *Biomaterials, 119*, 9–22.
8. Choi, D. S., Kim, D. K., Kim, Y. K., & Gho, Y. S. (2013). Proteomics, transcriptomics and lipidomics of exosomes and ectosomes. *Proteomics, 13*(10–11), 1554–1571.
9. Phinney, D. G., et al. (2015). Mesenchymal stem cells use extracellular vesicles to outsource mitophagy and shuttle microRNAs. *Nature Communications, 6*, 8472.
10. Maas, S. L. N., Breakefield, X. O., & Weaver, A. M. (2016). Extracellular Vesicles: Unique Intercellular Delivery Vehicles. *Trends in Cell Biology*. https://doi.org/10.1016/j.tcb.2016.11.003.
11. Witwer, K. W., et al. (2013). Standardization of sample collection, isolation and analysis methods in extracellular vesicle research. *Journal Extracell vesicles, 2*, 1–25.
12. Nickel, W. (2005). Unconventional secretory routes: Direct protein export across the plasma membrane of mammalian cells. *Traffic (Copenhagen, Denmark), 6*(8), 607–614.
13. Cocucci, E., Racchetti, G., & Meldolesi, J. (2009). Shedding microvesicles: artefacts no more. *Trends in Cell Biology, 19*(2), 43–51.
14. Mathivanan, S., Ji, H., & Simpson, R. J. (2010). Exosomes: Extracellular organelles important in intercellular communication. *Journal of Proteomics, 73*(10), 1907–1920.
15. Raposo, G., & Stoorvogel, W. (2013). Extracellular vesicles: Exosomes, microvesicles, and friends. *The Journal of Cell Biology, 200*(4), 373–383.
16. Kowal, J., et al. (2016) Proteomic comparison defines novel markers to characterize heterogeneous populations of extracellular vesicle subtypes. *Proceedings of the National Academy of Sciences of the United States of America* 113(8):E968-77.
17. Sorkin, A., & von Zastrow, M. (2002). Signal transduction and endocytosis: close encounters of many kinds. *Nature Reviews. Molecular Cell Biology, 3*(8), 600–614.
18. Scita, G., & Di Fiore, P. P. (2010). The endocytic matrix. *Nature, 463*(7280), 464–473.
19. Dobrowolski, R., & De Robertis, E. M. (2011). Endocytic control of growth factor signalling: multivesicular bodies as signalling organelles. *Nature Reviews Molecular Cell Biology, 13*(1), 53–60.
20. Li, L., et al. (2010). A unique interplay between Rap1 and E-cadherin in the endocytic pathway regulates self-renewal of human embryonic stem cells. *Stem cells (Dayton, Ohio), 28*(2), 247–257.
21. Théry, C., Amigorena, S., Raposo, G., & Clayton, A. (2006). Isolation and characterization of exosomes from cell culture supernatants and biological fluids. *Current Protocols in Cell Biology Chap, 3*, Unit 3.22.
22. Zanata, S. M., et al. (2002). Stress-inducible protein 1 is a cell surface ligand for cellular prion that triggers neuroprotection. *EMBO Journal, 21*(13), 3307–3316.
23. Kobayashi, T., et al. (2002). Separation and characterization of late endosomal membrane domains. *The Journal of Biological Chemistry, 277*(35), 32157–32164.
24. Bissig, C., & Gruenberg, J. (2013). Lipid sorting and multivesicular endosome biogenesis. *Cold Spring Harbor Perspectives in Biology, 5*(10), a016816.

25. Hurley, J. H., & Hanson, P. I. (2010). Membrane budding and scission by the ESCRT machinery: it's all in the neck. *Nature Reviews. Molecular Cell Biology, 11*(8), 556–566.
26. Hanson, P. I., & Cashikar, A. (2012). Multivesicular Body Morphogenesis. *Annual Review of Cell and Developmental Biology, 28*(1), 337–362.
27. Wollert, T., Wunder, C., Lippincott-schwartz, J., Hurley, J. H. (2009). Membrane scission by the ESCRT-III complex. *Nature, 458*(7235), 172–177.
28. Stenmark, H. (2009). Rab GTPases as coordinators of vesicle traffic. *Nature Reviews. Molecular Cell Biology, 10*(8), 513–525.
29. Villarroya-Beltri, C., Baixauli, F., Gutiérrez-Vázquez, C., Sánchez-Madrid, F., & Mittelbrunn, M. (2014). Sorting it out: Regulation of exosome loading. *Seminars in Cancer Biology, 28*(1), 3–13.
30. Kobayashi, T., et al. (1998). A lipid associated with the antiphospholipid syndrome regulates endosome structure and function. *Nature, 392*(6672), 193–197.
31. Bissig, C., & Gruenberg, J. (2014). ALIX and the multivesicular endosome: ALIX in Wonderland. *Trends in Cell Biology, 24*(1), 19–25.
32. Hajj, G. N. M., et al. (2013). The unconventional secretion of stress-inducible protein 1 by a heterogeneous population of extracellular vesicles. *Cellular and Molecular Life Sciences, 70*(17), 3211–3227.
33. Filipczyk, A., et al. (2015). Network plasticity of pluripotency transcription factors in embryonic stem cells. *Nature Cell Biology, 17*(10), 1235–1246.
34. Bernadskaya, Y., & Christiaen, L. (2016). Transcriptional Control of Developmental Cell Behaviors. *Annual Review of Cell and Developmental Biology, 32*(1), 77–101.
35. Tsanov, K. M., et al. (2016). LIN28 phosphorylation by MAPK/ERK couples signalling to the post-transcriptional control of pluripotency. *Nature Cell Biology*. https://doi.org/10.1038/ncb3453.
36. Acharya, D., et al. (2017). KAT-Independent Gene Regulation by Tip60 Promotes ESC Self-Renewal but Not Pluripotency. *Cell Reports, 19*(4), 671–679.
37. Kalkan, T., et al. (2017). Tracking the embryonic stem cell transition from ground state pluripotency. *Development (Cambridge, England), 144*(7), 1221–1234.
38. Ratajczak, J., et al. (2006). Embryonic stem cell-derived microvesicles reprogram hematopoietic progenitors: evidence for horizontal transfer of mRNA and protein delivery. *Leukemia: official journal of the Leukemia Society of America, Leukemia Research Fund, U. K, 20*(5), 847–856.
39. Lakkaraju, A., & Rodriguez-Boulan, E. (2008). Itinerant exosomes: emerging roles in cell and tissue polarity. *Trends in Cell Biology, 18*(5), 199–209.
40. Yuan, A., et al. (2009). Transfer of MicroRNAs by Embryonic Stem Cell Microvesicles. *PLoS One, 4*(3), e4722.
41. Khan, M., et al. (2015). Embryonic Stem Cell-Derived Exosomes Promote Endogenous Repair Mechanisms and Enhance Cardiac Function Following Myocardial Infarction. *Circulation Research, 117*(1), 52–64.
42. Murk, J. L., Stoorvogel, W., Kleijmeer, M. J., & Geuze, H. J. (2002). The plasticity of multivesicular bodies and the regulation of antigen presentation. *Seminars in Cell & Developmental Biology, 13*(4), 303–311.
43. Von Bartheld, C. S., & Altick, A. L. (2011). Multivesicular bodies in neurons: Distribution, protein content, and trafficking functions. *Progress in Neurobiology, 93*(3), 313–340.
44. Nichols, J., & Smith, A. (2012). Pluripotency in the embryo and in culture [review]. *Cold Spring Harbor Perspectives in Biology, 4*(8), 1–14.
45. Williams, R. L., et al. (1988). Myeloid leukaemia inhibitory factor maintains the developmental potential of embryonic stem cells. *Nature, 336*(6200), 684–687.
46. Raz, R., Lee, C. K., Cannizzaro, L. A., d'Eustachio, P., & Levy, D. E. (1999) Essential role of STAT3 for embryonic stem cell pluripotency. *Proceedings of the National Academy of Sciences of the United States of America* 96(6):2846–51.
47. Xu, H., Ang, Y.-S., Sevilla, A., Lemischka, I. R., & Ma'ayan, A. (2014). Construction and validation of a regulatory network for pluripotency and self-renewal of mouse embryonic stem cells. *PLoS Computational Biology, 10*(8), e1003777.
48. Sinha, A., Khadilkar, R. J., Vinay, K. S., Sinha, A. R., & Inamdar, M. S. (2013). Conserved regulation of the JAK/STAT pathway by the endosomal protein asrij maintains stem cell potency. *Cell Reports, 4*(4), 649–658.
49. Ying, Q.-L., et al. (2008). The ground state of embryonic stem cell self-renewal. *Nature, 453*(May), 519–523.
50. Dunn, S.-J., Martello, G., Yordanov, B., Emmott, S., & Smith a, G. (2014). Defining an essential transcription factor program for naïve pluripotency. *Science, 344*(6188), 1156–1160.
51. Taelman, V. F., et al. (2010). Wnt Signaling Requires Sequestration of Glycogen Synthase Kinase 3 inside Multivesicular Endosomes. *Cell, 143*(7), 1136–1148.
52. Roxrud, I., Stenmark, H., & Malerød, L. (2010). ESCRT & Co. *Biology of the Cell, 102*(5), 293–318.
53. Henne, W. M., Buchkovich, N. J., & Emr, S. D. (2011). The ESCRT Pathway. *Developmental Cell, 21*(1), 77–91.
54. Matsuo, H., et al. (2004). Role of LBPA and Alix in multivesicular liposome formation and endosome organization. *Science, 303*(5657), 531–534.
55. Falguières, T., Luyet, P. P., Bissig, C., Scott, C. C., Velluz, M. C., & Gruenberg, J. (2008). In vitro budding of intralumenal vesicles into late endosomes is regulated by Alix and Tsg101. *Molecular Biology of the Cell, 19*(11), 4942–4955. https://doi.org/10.1091/mbc.E08-03-0239.
56. Denzer, K., et al. (2000). Follicular dendritic cells carry MHC class II-expressing microvesicles at their surface. *Journal of Immunology, 165*, 1259–1265.
57. Wubbolts, R., et al. (2003). Proteomic and biochemical analyses of human B cell-derived exosomes: Potential implications for their function and multivesicular body formation. *The Journal of Biological Chemistry, 278*(13), 10963–10972.
58. Lässle, M., Blatch, G. L., Kundra, V., Takatori, T., & Zetter, B. R. (1997). Stress-inducible, murine protein mSTI1: Characterization of binding domains for heat shock proteins and in vitro phosphorylation by different kinases. *The Journal of Biological Chemistry, 272*(3), 1876–1884.
59. Lee, C.-T., Graf, C., Mayer, F. J., Richter, S. M., & Mayer, M. P. (2012). Dynamics of the regulation of Hsp90 by the co-chaperone Sti1. *The EMBO Journal, 31*(6), 1518–1528.
60. Schmid, A. B., et al. (2012). The architecture of functional modules in the Hsp90 co-chaperone Sti1/Hop. *The EMBO Journal, 31*(6), 1506–1517.
61. Lancaster, G. I., & Febbraio, M. A. (2005). Exosome-dependent trafficking of HSP70: A novel secretory pathway for cellular stress proteins. *The Journal of Biological Chemistry, 280*(24), 23349–23355.
62. McCready, J., et al. (2010). Secretion of extracellular hsp90α via exosomes increases cancer cell motility: a role for plasminogen activation. *BMC cancer, 10*(1), 294.
63. Longshaw, V. M., Baxter, M., Prewitz, M., & Blatch, G. L. (2009). Knockdown of the co-chaperone Hop promotes extranuclear accumulation of Stat3 in mouse embryonic stem cells. *European Journal of Cell Biology, 88*(3), 153–166.
64. Prinsloo, E., Setati, M. M., Longshaw, V. M., & Blatch, G. L. (2009) Chaperoning stem cells: A role for heat shock proteins

in the modulation of stem cell self-renewal and differentiation?. *BioEssays* 31(4):370–377.
65. Setati, M. M., et al. (2010). Leukemia inhibitory factor promotes Hsp90 association with STAT3 in mouse embryonic stem cells. *IUBMB Life, 62*(1), 61–66.
66. Yuan, A., et al. (2009) Transfer of microRNAs by embryonic stem cell microvesicles. PLoS One 4(3). https://doi.org/10.1371/journal.pone.0004722.
67. Katsman, D., Stackpole, E. J., Domin, D. R., & Farber, D. B. (2012). Embryonic stem cell-derived microvesicles induce gene expression changes in Müller cells of the retina. *PLoS One, 7*(11), e50417.
68. Dudu, V., Pantazis, P., & González-Gaitán, M. (2004). Membrane traffic during embryonic development: Epithelial formation, cell fate decisions and differentiation. *Current Opinion in Cell Biology, 16*(4), 407–414.
69. Matusek, T., et al. (2014). The ESCRT machinery regulates the secretion and long-range activity of Hedgehog. *Nature, 516*(7529), 99–103.
70. Zhang, L., & Wrana, J. L. (2014). The emerging role of exosomes in Wnt secretion and transport. *Current Opinion in Genetics & Development, 27*, 14–19.
71. Parchure, A., Vyas, N., Ferguson, C., Parton, R. G., & Mayor, S. (2015). Oligomerization and endocytosis of Hedgehog is necessary for its efficient exovesicular secretion. *Molecular Biology of the Cell, 26*(25), 4700–4717.
72. Rogers, K. W., & Schier, A. F. (2011). Morphogen Gradients: From Generation to Interpretation. *Annual Review of Cell and Developmental Biology, 27*(1), 377–407.
73. Wilcockson, S. G., Sutcliffe, C., & Ashe, H. L. (2016). Control of signaling molecule range during developmental patterning. *Cellular and Molecular Life Sciences*. https://doi.org/10.1007/s00018-016-2433-5.
74. Desrochers, L. M., Bordeleau, F., Reinhart-King, C. A., Cerione, R. A., & Antonyak, M. A. (2016). Microvesicles provide a mechanism for intercellular communication by embryonic stem cells during embryo implantation. *Nature Communications, 7*, 11958.
75. McGough, I. J., & Vincent, J.-P. (2016). Exosomes in developmental signalling. *Development (Cambridge, England), 143*(14), 2482–2493.
76. Sheldon, H., et al. (2010). New mechanism for Notch signaling to endothelium at a distance by delta-like 4 incorporation into exosomes. *Blood, 116*(13), 2385–2394.
77. Sharghi-Namini, S., Tan, E., Ong, L.-L.S., Ge, R., & Asada, H. H. (2014). Dll4-containing exosomes induce capillary sprout retraction in a 3D microenvironment. *Science Reporter, 4*, 4031.
78. Gross, J. C., Chaudhary, V., Bartscherer, K., & Boutros, M. (2012). Active Wnt proteins are secreted on exosomes. *Science Reporter, 14*(10), 1036–1045.
79. Chen, Y., et al. (2017). Aberrant low expression of p85α in stromal fibroblasts promotes breast cancer cell metastasis through exosome-mediated paracrine Wnt10b. *Oncogene, 36*(33), 4692–4705.